

Nucleon pairing in μ - capture by ^{40}Ca

Martoff, C. J.; Cummings, W. J.; Poanić, D.; Hanna, S. S.; Ullrich, H.; Furić, Miroslav; Petković, Tomislav; Kozłowski, T.; Perroud, J. P.

Source / Izvornik: **Physical Review C - Nuclear Physics, 1991, 43, 1106 - 1110**

Journal article, Published version

Rad u časopisu, Objavljena verzija rada (izdavačev PDF)

<https://doi.org/10.1103/PhysRevC.43.1106>

Permanent link / Trajna poveznica: <https://um.nsk.hr/um:nbn:hr:217:208301>

Rights / Prava: [In copyright](#)/[Zaštićeno autorskim pravom.](#)

Download date / Datum preuzimanja: **2024-07-17**



Repository / Repozitorij:

[Repository of the Faculty of Science - University of Zagreb](#)



Nucleon pairing in μ^- capture by ^{40}Ca

C. J. Martoff,* W. J. Cummings, D. Počanić,† and S. S. Hanna
Department of Physics, Stanford University, Stanford, California 94305

H. Ullrich

Institut für Experimentelle Kernphysik, University of Karlsruhe, Karlsruhe, Federal Republic of Germany

M. Furić

Faculty of Sciences, University of Zagreb, Zagreb, Yugoslavia

T. Petković

Faculty of Electrical Engineering, University of Zagreb, Zagreb, Yugoslavia

T. Kozłowski

*Institute for Nuclear Study, Swierk, Poland
 and Eidgenössische Technische Hochschule, Zürich, Switzerland*

J. P. Perroud

Institut de Physique Nucléaire, Lausanne, Switzerland

(Received 30 March 1990)

Spectra of energetic protons above 35 MeV have been measured following negative muon capture from rest in Ca. The spectrum extends to the kinematic limit near 93 MeV, with a branching ratio of $(2.3 \pm 0.3) \times 10^{-4}$ per capture above 40 MeV. Nuclear cascade calculations of the proton and neutron spectra in this energy region are presented and are consistent with the measured proton spectrum when capture on correlated pp and np pairs in the nucleus is included. The ratio of capture on np to pp pairs is 6.7 ± 1.6 , which is consistent with results from pion capture.

I. INTRODUCTION

It has been known for some time that in the capture of stopped negative muons by nuclei, neutrons are ejected with energies extending to the kinematic limit given by $(\mu^* - \Delta m) / [1 + m_n / m_{(Z-1, A-1)}]$.^{1,2} Here, μ^* is the effective muon mass, $m_\mu - m_e - \beta_\mu$, Δm is the nuclear Q value for $(Z, A) \rightarrow (Z-1, A-1) + n$, β_μ is the muon atomic binding energy, and the factor in the denominator accounts for the kinetic energy of the recoil nucleus. This limit is nearly 100 MeV (400 MeV/ c momentum) in typical cases.

Previous workers had found indications of energetic proton emission as well.²⁻⁴ Protons cannot be produced in this reaction as primary particles in one-body capture. Therefore, an accurate measurement of the proton spectrum could give information on the two- (or more-) body capture strength and the internal momentum spectrum of the correlations. Furthermore, pion absorption experiments have established an interesting systematic suppression of capture on isovector pp pairs relative to that on deuteronlike np pairs.⁵⁻⁹ If the same systematics were to be confirmed in muon capture, the exchange mechanism believed to be responsible for the pion capture systematics¹⁰ would be seen to be universal in axial-vector interactions with nucleon pairs. Therefore, the present work was undertaken to measure energetic proton spectra from

muon capture in several light- and medium-mass nuclei. We present below the results of measurements on ^{40}Ca .

II. EXPERIMENTAL METHOD

The experiment was performed at the Paul Scherrer Institute (PSI, formerly SIN) with the $\mu E4$ beam line. Negative muons of 50 MeV/ c momentum were stopped in a natural calcium target of about 300 mg/ cm^2 thickness inclined at 25° to the incident beam. The stopping rate was up to 10^5 per second in a spot of area $2 \times 5 \text{ cm}^2$. A stopped muon was tagged with pulses from three beam scintillators ($B1-B3$ in Fig. 1) which formed a box completely surrounding the target. The scintillator $B2$ (2 mm thick) was shaped to provide four sides of the box; scintillators $B1$ and $B3$ (both 1 mm thick) completed the enclosure as shown. The stopped muon was defined by a pulse from a particle passing through $B1$ (1 mm thick) and vetoed by signals in $B2$ and $B3$ (1 mm thick). The scintillators $B1-B3$ served the dual purpose of reliably identifying beam particles stopping in the target (while rejecting scattered beam particles) and identifying charged particles detected in the proton telescope that originated in the target (see below). The pion contamination in the stopping muon beam was measured to be less than 10^{-4} per stopped muon.

Charged particles from the target were detected in an

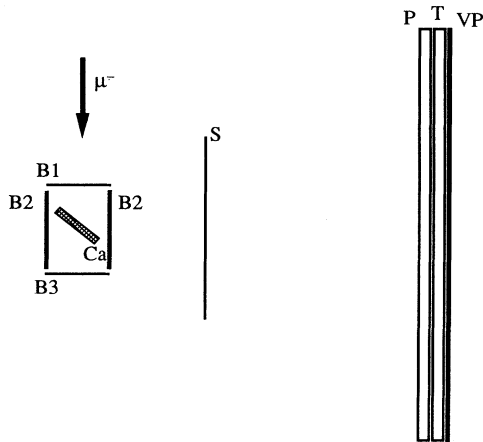


FIG. 1. The experimental arrangement. The scintillators $B1$ – $B3$ make up a box surrounding the target. The scintillators S , P , T and VP are elements of a charged-particle telescope.

extended telescope of plastic ($BC\ 408$) scintillators consisting of a 1-mm-thick detector (S), a 60-cm air gap, a pair of 35-mm-thick detectors mounted side by side (P), a further pair of 35-mm-thick detectors (T), and a pair of veto detectors (VP) behind T . Protons were identified by the $\Delta E/E$ method applied to S and P and P and T , as well as by checking their S to P time of flight against the deposited energy. As a further check, the time of each accepted event relative to the stopped muon signal was measured to verify that identified protons showed the lifetime characteristic of muons decaying and capturing in the target material. Charged particles detected in fast coincidence with a pulse in $B1$ or $B3$ (“prompts”) were tagged for off-line rejection, since these events were likely to have come from pion capture rather than muon capture. Events accepted in the proton telescope were gated by pulses from $B2$ to ensure that these events originated in the target. The telescope thickness, not including VP , was sufficient to stop protons with energy about equal to the muon rest mass. The telescope was also fully efficient for protons above 35 MeV because at this energy a proton was able to escape the target, traverse S , and just leave a detectable signal in the P detectors.

Of the Michel electrons from muon decays in the target, 90% penetrated into VP and were vetoed. Energy calibration of the charged-particle detector (S - P - T - VP) was performed on a sample of the penetrating Michel electrons. This calibration was checked with pulses from protons just stopping in the P detectors. These calibration protons were produced from pion capture on carbon.¹¹ In the muon reaction, the yield of protons was normalized by dividing it by the number of muon captures, which was calculated by multiplying the number of muons stops (as observed by the beam detectors) by the known capture branching ratio.¹² The number of muon captures was corrected for several effects, including computer dead time, events falsely rejected as prompt, and those in which the muon is no longer present during the gate because of its decay lifetime. The error in this normalization measurement is about 10%. The number of

captures was checked by comparison to the number of (prescaled) Michel electrons observed (and hence to the number of muon decays). The two calculations agreed within 10%. The pulse-height spectrum from decay electrons passing through the charged-particle detectors was compared to an EGS code simulation¹³ to determine the energy resolution of the charged-particle detectors. The calibration protons mentioned above were also used to determine this resolution, which was found to be 25% FWHM for 70 MeV protons.

III. RESULTS

The energy spectrum of protons emitted following muon capture in ^{40}Ca as measured by the proton telescope (without corrections) is shown in Fig. 2. First, it was assumed that the emitted proton energy spectrum has the following energy dependence:

$$\frac{d\Gamma}{d\Gamma_p} = C e^{-\langle T_p/T_0 \rangle}, \quad (1)$$

as has been customary in previous works.^{1,3,4,14} The curve generated by this expression was corrected for energy losses in the target and the material between the target and the P detector was modified by folding in the energy resolution function and then was fitted to the histogram in Fig. 2 using statistical errors only. The result is shown as the solid curve in Fig. 2. The fit gives $C = (4.5 \pm 0.2) \times 10^{-3} \text{ MeV}^{-1}$ (where the error is statistical only and does not include the normalization error) and $T_0 = 8.0 \pm 1.5 \text{ MeV}$ and a branching ratio (number of emitted protons per μ^- capture) between 40 and 92.7 MeV of 2.35×10^{-4} . This shape gives a reasonable fit below 60 MeV but overestimates the spectrum at the highest energies.

A second fit was obtained with the formula

$$\frac{d\Gamma}{d\Gamma_p} = C E_\nu^2 e^{-\langle T_p/T_0 \rangle}, \quad (2)$$

where the neutrino energy (E_ν) is calculated on the assumption that the recoil nucleus is ^{39}Ar in the ground state. This second shape attempts to include the phase-space cutoff at the kinematic limit. This shape after correction is shown as the dashed line in Fig. 2. In this case the fit gives $C = (2.4 \pm 0.1) \times 10^{-7} \text{ MeV}^{-3}$ and $T_0 = 12.3 \pm 1.0 \text{ MeV}$ and a branching ratio between 40 and 92.7 MeV of 2.32×10^{-4} . Thus, the branching ratio is virtually unchanged in this second fit and agrees very well with the value of 2.5×10^{-4} for protons above 39.5 MeV previously reported for μ^- capture on ^{40}Ca ,³ as extracted from 20 events.

IV. DISCUSSION

It is important to determine whether a significant portion of the observed protons could be due to cascading by neutron and proton decays following the initial capture process. The Livermore code¹⁵ ALICE was used to calculate the secondary proton spectrum expected to accompany the neutrons observed in Ref. 1. This proton spectrum was then compared to the present results. ALICE is

a hybrid-model cascade code which has been extensively validated with nucleon- and heavy-ion-induced reaction data, as well as with pion capture data.¹⁶ We shall refer to particles emitted promptly with the capture process as primary particles and those resulting from subsequent cascading as secondary particles, although the distinction at early times is not always clear cut.

The neutron energy spectrum from muon capture in Ca,¹ shown in Fig. 3, was fitted with ALICE in the following way. Cascades were generated that started with primary neutron emissions sorted into kinetic energy bins covering 20 to 92.7 MeV. The resulting emitted spectra for the energy bins were summed with energy-dependent factors chosen so that above 35 MeV the total neutron yield would fit the experimental neutron spectrum, taking into account also the neutrino phase space. The fit to the neutron spectrum achieved in this way is shown as the solid line in Fig. 3. The secondary proton spectrum corresponding to this ALICE fit to the neutron data, corrected for energy losses before entering the detector and the energy resolution of the detector, is shown by the long-short dashed curve in Fig. 2. This predicted proton contribution falls short of the experimental data by an energy-dependent factor of between 2 and 4. The model used in this calculation is a one neutron-particle, one proton-hole configuration (*nh*) that results from a simple one-body muon capture mechanism. It gives the largest number of energetic secondary protons of any initial configuration not containing primary protons.

A similar procedure was followed for cascades initiated from a two neutron-particles, one highly correlated proton-hole configuration (*nnh*).¹⁶ This configuration is intended to model two-body capture on correlated *np* pairs as the source of the energetic neutrons. The resulting proton spectrum (not shown) is slightly softer than for the *nh* case, falling even farther short of the data. Quantitatively, these results indicate that more than 50% of the protons observed above 40 MeV are primary protons. Since primary protons cannot be produced in a one-body μ^- capture, we associate these primary protons with capture on correlated *pp* pairs from which it is the “spectator” protons that are emitted and observed. If one assumes that the pairs are nearly at rest in the nucleus, their internal relative momenta would need to provide the momenta of the emitted protons. For the first time these results establish a two-body mechanism of proton production in muon capture, independently of arguments about the reasonableness of high-momentum wave-function components.

To compare the present result with pion capture (in which energetic nucleon emission is also dominated by a pair capture mechanism), it is of interest to estimate the ratio *R* of μ^- captures on *np* to *pp* pairs. This is traditionally done directly from the data by neglecting nuclear scattering entirely, giving⁸

$$R(T_{\text{cutoff}}) = \frac{\Gamma_n - \Gamma_p}{2\Gamma_p}, \quad (3)$$

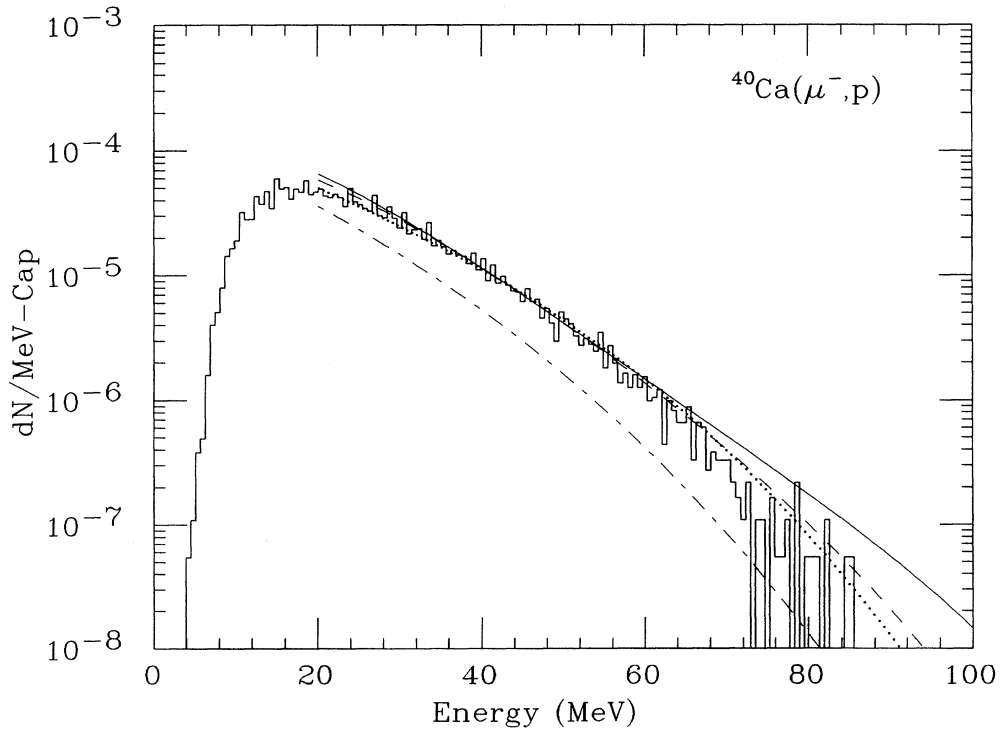


FIG. 2. The histogram shows the measured proton energy spectrum (without corrections) for the reaction $^{40}\text{Ca}(\mu^-, p)$. The solid and dashed curves represent phenomenological fits explained in the text. The long-short dashed curve is the proton result when the neutron spectrum (Fig. 3) is fitted with weighted cascades from an *nh* configuration. The dotted curve results when an *nnh* configuration is used. See text.

where $\Gamma_{n(p)}$ is the branching ratio for neutrons (protons) above a cutoff energy T_{cutoff} . Combining the present result with that of Ref. 1 gives $R = 6.7 \pm 1.6$ for muon capture with a cutoff of 40 MeV. As noted by pion capture authors,⁸ Eq. (3) represents a strict lower limit on the value of R . Unfortunately, whereas a pion capture spectrum for $^{40}\text{Ca}(\pi^-, p)$ has been obtained,⁷ the corresponding $^{40}\text{Ca}(\pi^-, n)$ spectrum has not, so it is not possible to compare directly our result to the corresponding pion capture result. Pion capture measurements have been made for the ^{59}Co nucleus⁷ with a result of $R = 2.2 \pm 0.7$; however, at least one author¹⁶ comments that the high-energy yield for protons from ^{59}Co is unusually high when compared to other nuclei.

To calculate the value of R when secondary cascading is included, a model was chosen in which all captures (which lead to energetic nucleon emission) occurred on correlated pairs. The ratio R is then calculated directly from that ratio of np captures to pp captures that best fits the data. The calcium data are best fitted by a combination of 94% np captures (cascading modeled by an nnh configuration ALICE calculation) and 6% pp captures (cascading modeled by an nph ALICE calculation). This fit to the neutron spectrum is shown as the dashed line in Fig. 3. The corresponding proton spectrum result, shown in Fig. 2 as a dotted line, fits the experimental histogram rather well. These calculations given an R of 16 ± 1 for

the initial capture distribution. This procedure is to be compared with a similar one used for pion capture by Chiang and Hufner⁶ to predict the $^{40}\text{Ca}(\pi^-, p)$ spectrum as measured by Randoll *et al.*⁷ The first authors used an input value of R of 4.25 and overestimated the number of high-energy protons. The ALICE code was used by Blann¹⁶ to predict the same spectrum and he obtained reasonable (within his stated accuracy of $\pm 20\%$) results for R between 9 and 20.

All the above arguments lead one to understand muon capture at large energy transfer by recognizing the presence of an interaction of the capturing muon with correlated pairs of nucleons. Indeed, direct coincidence measurements of nn (Ref. 14) and np (Ref. 17) final states confirm this picture. In summary, a detailed pre-equilibrium cascade treatment of high-energy protons emitted following muon capture in ^{40}Ca shows a strong enhancement of protons over what one would expect simply from secondary cascading of neutrons and protons. These primary protons can be explained by the presence of a two-body capture mechanism (similar to that for π capture) with a large suppression of captures on pp pairs in comparison with pn pairs (see values of R obtained above). Two-nucleon correlations in nuclei have been the subject of considerable interest and controversy. Of special importance are the roles played by different probes in observing nucleon pairing. The present muon capture ex-

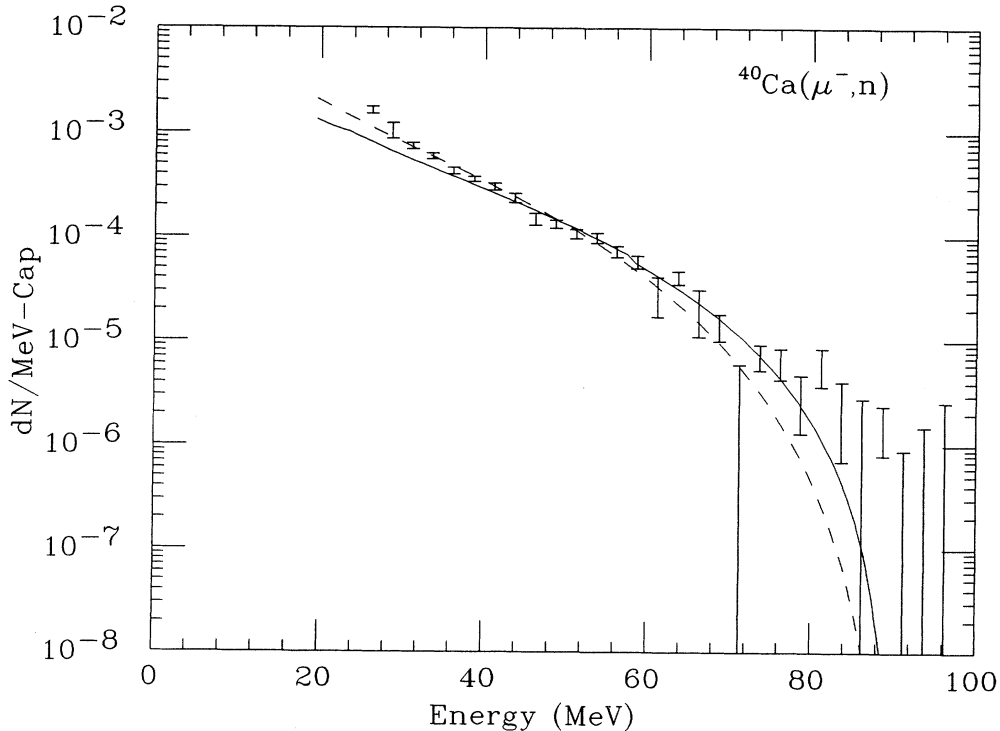


FIG. 3. The histogram shows the neutron spectrum for the reaction $^{40}\text{Ca}(\mu^-, n)$ (Ref. 1). The solid and dashed curves are ALICE fits to the spectrum with weighted cascades from an nh and nnh configuration, respectively. See corresponding proton curves in Fig. 2 and also text.

periment provides yet another result that must be accommodated by a successful model of nucleon pairing in the nuclear medium.

ACKNOWLEDGMENTS

We wish to thank Marshall Blann and Sebastian Kuhn for valuable discussions. We gratefully acknow-

ledge the Pew Foundation for providing the computer facility used in the analyses in this work. We also thank K. Gabathuler of the electronics pool and the cyclotron crew of the Paul Scherrer Institute for their generous help in carrying out the experiment. The research was supported in part by the U.S. National Science Foundation.

*Present address: Physics Department, Temple University, Philadelphia, PA 19122.

†Present address: Physics Department, University of Virginia, Charlottesville, VA 22901.

¹J. van der Pluym, T. Kozłowski, W. H. A. Hesselink, A. van der Schaaf, Ch. Grab, E. A. Hermes, and W. Bertl, *Phys. Lett. B* **177**, 21 (1986).

²References to earlier work are given in reviews by P. Singer, *Springer Tracts Mod. Phys.* **71**, 39 (1974); N. C. Mukhopadhyay, *Phys. Rep.* **30C**, 1 (1977); Y. A. Batusov and R. A. Eramzhyan, *Fiz. Elem. Chastits At. Yadra* **8**, 220 (1977) [*Sov. J. Part. Nucl.* **8**, 92 (1977)].

³Y. G. Budyashov, V. G. Zinov, A. D. Konin, A. I. Mukhin, and A. M. Chatrchyan *Zh. Eksp. Teor. Fiz.* **60**, 19 (1971) [*Sov. Phys. JETP* **33**, 11 (1971)]; M. P. Balandin, V. M. Grebenyuk, V. G. Zinov, T. Kozłowski, and A. D. Konin, *Yad. Fiz.* **28**, 582 (1978) [*Sov. J. Nucl. Phys.* **28**, 297 (1978)].

⁴K. S. Krane, T. C. Sharma, L. W. Swenson, D. K. McDaniels, P. Varghese, B. E. Wood, R. R. Silbar, H. D. Wohlfahrt, and C. A. Goulding, *Phys. Rev. C* **20**, 1873 (1979).

⁵Pion capture data can be found in the following references: C. E. Stronach, B. J. Lieb, H. O. Funsten, W. J. Kossler, H. S. Plendl, and V. G. Lind, *Phys. Rev. C* **23**, 2150 (1981); R. Hartmann, H. P. Isaak, R. Engfer, E. A. Hermes, H. S. Pruys, W. Dey, H. J. Pfeiffer, U. Sennhauser, H. K. Walter, and J. Morgenstern, *Nucl. Phys.* **A308**, 345 (1978); U. Sennhauseer, H. J. Pfeiffer, H. K. Walter, F. W. Schlepütz, H. S. Pruys, R. Engfer, E. A. Hermes, P. Heusi, H. P. Isaak, and W. H. A. Hesselink, *ibid.* **A386**, 429 (1982); P. Heusi, H. P. Isaak, H. S. Pruys, R. Engfer, E. A. Hermes, T. Kozłowski, U. Sennhauser, and H. K. Walter, *ibid.* **A407**, 429 (1983).

⁶H. C. Chiang and J. Hüfner, *Nucl. Phys.* **A352**, 442 (1981).

⁷H. Randall, H. I. Amols, W. Kluge, H. Matthay, A. Moline, and D. Münchmeyer, *Nucl. Phys.* **A381**, 317 (1982).

⁸H. S. Pruys, R. Engfer, R. Hartmann, E. A. Hermes, H. P.

Isaak, F. W. Schlepütz, U. Sennhauser, W. Dey, K. Hess, H.-J. Pfeiffer, H. K. Walter, and W. Hesselink, *Nucl. Phys.* **A352**, 388 (1981); M. E. Nordberg, K. F. Kinsey, and R. L. Bruman, *Phys. Rev.* **165**, 1096 (1968).

⁹B. Gotta, M. Dorr, W. Fetcher, G. Schmidt, H. Ullrich, G. Backenstoss, W. Kowald, I. Schwanner, and H. J. Weyer, *Phys. Lett.* **112B**, 129 (1981); G. Backenstoss, W. Kowald, I. Schwanner, H. J. Weyer, M. Dorr, D. Gotta, G. Schmidt, L. M. Simons, and H. Ullrich, *ibid.* **115B**, 445 (1982).

¹⁰D. S. Koltun and A. Reitan, *Phys. Rev.* **141**, 1413 (1966); **155**, 1139 (1967); D. Ashery, R. J. Holt, H. E. Jackson, J. P. Schiffer, J. R. Specht, K. E. Stephenson, R. D. McKeown, J. Ungar, R. E. Segel, and P. Zupranski, *Phys. Rev. Lett.* **47**, 895 (1981); K. Ohta, M. Thies, and T. S. H. Lee, *Ann. Phys. (N.Y.)* **163**, 420 (1985).

¹¹G. Mechttersheimer, G. Büche, U. Klein, W. Kluge, H. Matthäy, D. Münchmeyer, and A. Moline, *Phys. Lett.* **73B**, 115 (1978).

¹²M. Eckhause, R. T. Siegel, R. E. Welsh, and T. A. Filippas, *Nucl. Phys.* **81**, 575 (1966).

¹³D. W. O. Rogers, *Nucl. Instrum. Methods* **A227**, 535 (1984).

¹⁴A. van der Schaaf, E. A. Hermes, R. J. Powers, F. D. Schlepütz, R. G. Winter, A. Zglinski, T. Kozłowski, W. Bertl, F. Felawka, W. H. A. Hesselink, and J. van der Pluym, *Nucl. Phys.* **A408**, 573 (1983); T. Kozłowski, W. Bertl, H. P. Povel, U. Sennhauser, H. K. Walter, A. Zglinski, R. Engfer, Ch. Grab, E. A. Hermes, H. P. Isaak, A. van der Schaaf, J. van der Pluym, and W. H. A. Hesselink, *ibid.* **A436**, 717 (1985).

¹⁵M. Blann, *Annu. Rev. Nucl. Sci.* **25**, 123 (1975); LLNL Report UCID 19614, 1982.

¹⁶M. Blann, *Phys. Rev. C* **28**, 1648 (1983).

¹⁷W. J. Cummings, C. J. Martoff, D. Počanić, S. S. Hanna, H. Ullrich, M. Furić, T. Petković, T. Kozłowski, and J. P. Perroud (unpublished).